REPORT DOCUMENTATION PAGE

Form Approved
OMB No. 0704-0188

1. AGENCY USE ONLY (Leave blank)	2. REPORT DATE	3. REPORT TYPE AND DATES COVERED
		FINAL TECHNICAL - 15 May 95 - 14 May 96

4. TITLE AND SUBTITLE
OPTICAL AND MAGNETIC RESONANCE CHARACTERIZATION OF POINT DEFECTS IN NONLINEAR CRYSTALS

5. FUNDING NUMBERS
95HS28
95HS/281

6. AUTHOR(S)
Professor Halliburton

7. PERFORMING ORGANIZATION NAME(S) AND ADDRESS(ES)
Department of Physics
West Virginia University
Morgantown, WV 26506-6845

AFOSR-TR-97
0181

9. SPONSORING/MONITORING AGENCY NAME(S) AND ADDRESS(ES)
AFOSR/NE
110 Duncan Avenue Suite B115
Bolling AFB DC 20332-8080

10. SPONSORING/MONITORING AGENCY REPORT NUMBER
F49620-95-1-0349

11. SUPPLEMENTARY NOTES

12a. DISTRIBUTION/AVAILABILITY STATEMENT
APPROVED FOR PUBLIC RELEASE: DISTRIBUTION UNLIMITED

12b. DISTRIBUTION CODE

13. ABSTRACT (Maximum 200 words)

The research performed over one year was to use electron paramagnetic resonance (EPR), electron-nuclear double resonance (ENDOR), fourier-transform-infrared (FTIR) absorption, and other optical techniques to identify and characterize point defects in nonlinear optical materials. The materials studied were KTP, $ZnGeP_2$, and $CdGeAs_2$ families nonlinear optical crystals. Photoluminescence and micro-Raman techniques were found to be useful for clarifying the origin of near-infrared emission in, and characterizing the decomposition process at the surface of KTP crystals. EPR spectra of $ZnGeP_2$ indicate that near-edge optical absorption is dominated by singly-ionized zinc vacancies, and large concentrations of phosphorus vacancy donors were present as well. Photoluminescence studies further support that the optical absorption is likely due to several overlapping bands arising from an acceptor-to-donor transition and band-to-defect transitions.

14. SUBJECT TERMS			15. NUMBER OF PAGES
			16. PRICE CODE
17. SECURITY CLASSIFICATION OF REPORT	18. SECURITY CLASSIFICATION OF THIS PAGE	19. SECURITY CLASSIFICATION OF ABSTRACT	20. LIMITATION OF ABSTRACT
UNCLASSIFIED	UNCLASSIFIED	UNCLASSIFIED	

FINAL TECHNICAL REPORT

(For Period from May 15, 1995 to May 14, 1996)

TABLE OF CONTENTS

page

I. Executive Summary 1

II. Results of Point Defect Studies in KTP 2

III. Results of Point Defect Studies in $ZnGeP_2$.....6

References.....9

Figure Captions 12

Figures 13

I. EXECUTIVE SUMMARY

This document is a final technical report for work performed under Air Force Office of Scientific Research (AFOSR) Grant F49620-95-1-0349. The title of the project was "Optical and Magnetic Resonance Characterization of Point Defects in Nonlinear Crystals" and the Principal Investigator is Larry E. Halliburton, Physics Department, West Virginia University. The amount of the award was $19,971. This was a one-year research program to use electron paramagnetic resonance (EPR), electron-nuclear double resonance (ENDOR), fourier transform infrared (FTIR) absorption, and other optical techniques to identify and characterize point defects in the KTP, $ZnGeP_2$, and $CdGeAs_2$ families of nonlinear optical crystals. The grant's active period was from May 15, 1995 to May 14, 1996.

Work done under this project resulted in a paper published in Applied Physics Letters entitled "Photoluminescence and Micro-Raman Studies of As-Grown and High-Temperature-Annealed $KTiOPO_4$," (K. T. Stevens, N. C. Giles, and L. E. Halliburton, Appl. Phys. Lett. 68, 897, 1996) and in an oral presentation at the March 1996 Meeting of the American Physical Society in St. Louis. A 15-minute oral presentation entitled "Identification of Point Defects in $ZnGeP_2$ Crystals" was made at the AFOSR Semiconductor and Electromagnetic Materials Program Review at WPAFB on August 22, 1996.

II. RESULTS OF POINT DEFECT STUDIES IN KTP

Potassium titanyl phosphate ($KTiOPO_4$), better known as KTP, is a nonlinear optical material widely used in frequency conversion applications such as second-harmonic generation and optical parametric oscillation.[1] In many cases, however, the full potential of this material has not been achieved because of the presence of point or extended defects.[2-6] These defects may be introduced during crystal growth, during subsequent device fabrication, or during device operation. High laser powers, applied electric fields, reducing atmospheres, elevated temperatures, or other extreme conditions may initiate defect formation at the surface or in the bulk of KTP crystals.

We performed a detailed photoluminescence and micro-Raman study of KTP. Two important, and related, properties of this material are addressed, namely defect luminescence and surface decomposition. We have monitored a recently discovered[7] luminescence band which occurs near 820 nm at room temperature in crystals grown by the flux technique. Annealing in air at 1000°C for one hour greatly enhances this near-infrared emission (shifting its peak slightly to 835 nm) and simultaneously causes significant decomposition of the KTP surface. The anatase form of TiO_2 is left as the dominant component in the near-surface region after the 1000°C anneal. We attribute the emission near 835 nm to Ti^{3+} ions present in (or near) the TiO_2 surface layer. These ions are apparently formed during the strongly reducing conditions associated with the decomposition process. Based upon the results of the high-temperature anneal, we suggest that the 820-nm emission in as-grown KTP is due to Ti^{3+} ions present in micro-regions of reduced TiO_2 (either rutile or anatase) that form in the bulk of the KTP crystals during growth.

The series of KTP crystals used in the present study were grown by the flux technique at Crystal Associates, Waldwick, NJ. They had dimensions of a few mm on a side and their faces were perpendicular to the three high-symmetry crystallographic directions a, b, and c. Photoluminescence and micro-Raman data were obtained at room temperature using a Jobin-Yvon Ramanor U-1000 double monochromator with a microprobe attachment. A GaAs-cathode photomultiplier tube (Hamamatsu R943-02) and photon-counting electronics were employed to detect the signals. An Innova 400-10 argon-ion laser from Coherent provided the cw 457-nm excitation, while an Olympus BH-2 microscope focused the beam to a spot size of about 20 μm in diameter on the sample. The resulting power density on the sample surface was 1.9×10^3 W/cm^2. Because of the strong focusing effect of the microscope, the primary region of excitation and collection of luminescence did not extend more than approximately 50 to 100 μm into the sample. All

of the photoluminescence spectra were corrected for the wavelength-dependent response of the spectrometer and detector.

Figure 1 shows the room-temperature, near-infrared emission band detected from flux-grown KTP crystals when excited by 457-nm light. This band peaks near 820 nm and its intensity depends linearly on excitation power. Data from three as-grown samples are presented in Fig. 1. Trace (a) represents recent commercially available material while traces (b) and (c) represent material from early crystal-growth efforts (i.e., before many of the growth conditions were optimized). The low-energy side of the emission band was not recorded because of phototube limitations.

Three significant observations were initially made concerning this 820-nm emission band. First, the intensity of the emission is sample dependent, as illustrated in Fig. 1. Second, the source of the emission is uniformly distributed in as-grown crystals. Third, a limited survey of hydrothermally grown KTP suggests that this emission is either not present or is extremely weak in as-grown crystals of that type. In support of the second observation, a systematic variation of the position of the 20-μm-diameter excitation beam on a surface gave little change in emitted intensity. Also, a freshly exposed surface produced by fracturing a crystal, when examined less than one minute after fracture, gave the same emitted intensity as the original surface prepared months earlier by the manufacturer. These latter data verified that the emission from as-grown crystals is not simply a surface phenomenon that depends on the length of time a surface has been exposed to air at room temperature.

The most likely origin of the 820-nm emission band is Ti^{3+} ions. Recent studies of Ti^{3+} as a potential lasing ion in various host materials have shown that its emission often peaks near 800 nm while its absorption peaks in the 400 to 500 nm region.[8-10] In a cubic field, the ^2D state of this $3d^1$ ion is split into the threefold degenerate $^2T_2$ ground state and the twofold degenerate ^2E excited state. Reducing the symmetry of the Ti^{3+} site will further remove these degeneracies. The Stokes-shifted emission then occurs from the lower sublevel of the excited state to the ground state and its peak position depends directly on the strength of the crystal field.[11]

After the initial observations of this 820-nm band, efforts were made in our laboratory to enhance its intensity. Electron paramagnetic resonance (EPR) studies[5,12,13] previously have shown that large concentrations of Ti^{3+} ions can be produced in KTP by reducing treatments at elevated temperatures or by exposure to ionizing radiation at lower

temperatures. However, much to our surprise, we found that applying an electric field across a crystal at elevated temperature (in a manner similar to Roelofs[12]) did not change the intensity of the 820-nm emission even though the crystal was discolored and EPR experiments verified that a large concentration of Ti^{3+} ions had been formed. In separate investigations, we discovered that x-ray-irradiation, at 77 K or room temperature, also does not change the intensity of the 820-nm emission even though significant concentrations of Ti^{3+} ions were formed. Thus, we are led to the conclusion that the 820-nm emission does not result from the Ti^{3+} ions that are normally observed with EPR in the regular KTP lattice.

Following a different approach, we found that the intensity of the near-infrared emission increased by approximately two orders of magnitude when a KTP crystal was held for one hour at 1000°C in air. A micro-Raman spectrum taken at the same location as the photoluminescence revealed that the high-temperature anneal had caused significant decomposition at the KTP surface. Removal of the decomposed portion of the crystal surface by polishing returned the near-infrared emission and the micro-Raman spectra to their original (i.e., before anneal) intensities. This cycle of production by high-temperature anneal and removal by polishing verified that the enhancement of the emission band was occurring only in a region of the crystal near the surface.

Figures 2 and 3 illustrate the changes in the near-infrared emission and the micro-Raman spectra, respectively, that resulted from the one-hour anneal at 1000°C in air. For both types of data, the excitation beam was propagating along the c axis of the crystal with its electric field parallel to the a axis. The spectra taken before the high-temperature anneal are shown in Figs. 2(a) and 3(a), the spectra taken from one location on the surface after the 1000°C anneal are shown in Figs. 2(b) and 3(b), and the spectra taken from a different location on the surface after the anneal are shown in Figs. 2(c) and 3(c). An important feature in Fig. 2 is the small shift in the peak position of the emission from 820 nm before the high-temperature anneal to 835 nm after the anneal. We believe the same type of defect is still causing the emission, namely Ti^{3+}, but that its environment may be slightly different in the decomposing region. One purpose of showing data from two distinct locations on the crystal surface (i.e., traces b and c in Figs. 2 and 3) is to illustrate the nonuniformity of the decomposition rate across the surface. This nonuniform decomposition is probably associated with a slight unevenness in the original surface polish.

Comparison of the micro-Raman spectra before and after the high-temperature anneal reveal major changes. Fig. 3(a) represents the usual KTP spectrum with the most

intense Raman peak at 763 cm^{-1}. This peak is nearly gone in Figs. 3(b) and 3(c) and a spectrum having an intense peak at 143 cm^{-1} has appeared. The presence of the 143 cm^{-1} Raman peak clearly indicates that the anatase form of TiO_2 has been formed by the high-temperature anneal.[14-16] Hagerman et al.[17] have shown that KTP decomposes at elevated temperatures according to the following reaction

$$KTiOPO_4 \rightarrow (1-\alpha)KTiOPO_4(s) + \alpha TiO_2(s) + (\alpha/2)(P_2O_5 + K_2O)(g)$$

where α represents the extent of decomposition. Potassium, phosphorus, and oxygen leave the surface in the gas phase. Using x-ray diffraction, Hagerman et al.[17] determined that the solid form of TiO_2 remaining on the surface was rutile. In our investigation, using micro-Raman, we find the solid form of the remaining TiO_2 to be anatase. These results from the two groups do not necessarily conflict since the samples were maintained at high temperature for significantly different times in the two experiments (one hour in our present study versus tens of hours in the earlier work). In general, there are three polymorphs of TiO_2 which are stable at room temperature (rutile, anatase, and brookite). Anatase is known to convert to rutile on heating above about 915°C; however, numerous factors related to the possible topotaxy in both the decomposition process and the anatase-rutile transformation may affect the actual temperature range over which this phase change might occur on the surface of KTP crystals.

Returning to traces b and c in Figs. 2 and 3, we see that the intensity of the 835-nm emission correlates directly with the amount of TiO_2 (anatase) formed at a given location. These results, when coupled with the more general observation that decomposition of the surface is the only way to enhance the near-infrared emission, leave little doubt that the origin of this emission is Ti^{3+} ions in the TiO_2 layer produced during the high-temperature anneal. These Ti^{3+} ions would be expected to form as a result of the strongly reducing conditions associated with the decomposition process. Also, there is a known emission band peaking near 850 nm in crystalline TiO_2 (rutile) which further supports our assignment of the observed emission to defects in TiO_2.[18-21]

Our results have shown that the emission at 820 nm in the as-grown KTP crystals does not correlate in any manner with the Ti^{3+} ions that are produced in the regular KTP lattice by reducing treatments or ionizing radiation. Additional experiments showed that high-temperature decomposition of the KTP surface produced large concentrations of TiO_2 (anatase) and an accompanying large 835-nm emission. Together, these observations

suggest that the 820-nm emission band present in the crystals grown by the flux technique must be due to Ti^{3+} ions in micro-regions of TiO_2 (either rutile or anatase) that form in the bulk of the KTP crystals during growth. Why Ti^{3+} ions in the regular KTP lattice do not luminesce remains an open question.

To summarize, we demonstrated that photoluminescence and micro-Raman are useful techniques for characterizing KTP crystals. Their combined use has clarified the origin of the neaf-infrared emission in as-grown KTP crystals. Also, they provide a sensitive local probe to study the nature of the decomposition process at the surface of KTP. It is expected that these spectroscopic techniques will be especially useful in future studies of thin films of KTP.[6]

III. RESULTS OF POINT DEFECT STUDIES IN $ZnGeP_2$

In recent years, considerable progress has been made in the growth of high-quality zinc germanium phosphide ($ZnGeP_2$) crystals for use in frequency conversion applications in the mid-infrared. A suitable birefringence, a large nonlinear optical coefficient, and good thermal conductivity make this material an excellent choice for optical parametric oscillators (OPOs) tunable in the 3 to 9 μm region. However, before $ZnGeP_2$ can achieve its full potential, a broad defect-related absorption band extending from 0.7 to 2.5 μm must be eliminated. This unwanted absorption band overlaps the desirable 2-μm pump region for mid-infrared OPOs and thus limits the maximum pump intensity that can be used in these devices. Several post-growth methods to reduce this absorption have been investigated, including lengthy thermal anneal, high-energy electron irradiation,[22] and gamma-ray irradiation.[23] These treatments, although helpful, have not eliminated the absorption problem in $ZnGeP_2$.

Nearly all of the $ZnGeP_2$ crystals described in the literature have been highly compensated, thus indicating nearly equal concentrations of donors and acceptors. There are two competing explanations for the nature of these donors and acceptors. One approach is to assume these defects arise from disorder on the zinc and germanium sublattices, i.e., a zinc antisite defect would be an acceptor and a germanium antisite would be a donor. An alternate approach is to assume that the donors and acceptors are vacancy centers. Magnetic resonance techniques such as EPR, ENDOR, and ODMR make use of hyperfine interactions to identify specific defect models and thus can help to determine whether cation disorder or vacancies dominate in $ZnGeP_2$. Thus far, the zinc

vacancy,[24] the phosphorus vacancy,[25] and the phosphorus antisite[26] have been detected by EPR.

The $ZnGeP_2$ crystals used in the present investigation were grown by the horizontal gradient freeze technique at Sanders, a Lockheed Martin Company. Small samples with approximate dimensions of 3 x 3 x 3 mm^3 were cut from larger boules. They had faces perpendicular to the high symmetry directions. The EPR data were taken on a Bruker ESP-300 spectrometer operating at 9.45 GHz and equipped with an Oxford Instruments helium-gas-flow cryostat for low temperature studies. Slots in the EPR microwave cavity allowed optical access to the samples. In the photoluminescence (PL) measurements, both cw (514.5-nm argon laser) and pulsed (532-nm frequency-doubled Nd:YAG laser) excitation were used. The PL signals were detected with an Instruments SA HR-640 monochromator and a photomultiplier tube with a GaAs(Cs) cathode. For cw excitation, the incident beam was chopped and phase-sensitive detection was used. Time-decay data were recorded using a Tektronix (TDS 684A) digital oscilloscope.

EPR shows the presence of two dominant native defects, a zinc vacancy and a phosphorus vacancy, in all of the $ZnGeP_2$ samples grown by the horizontal gradient freeze technique. The singly ionized zinc vacancy acceptor is paramagnetic ($S = ½$) and is easily seen without photoexcitation at temperatures below 50 K.[24] The unpaired spin is shared nearly equally by two phosphorus nuclei ($I = ½$, 100% abundant), which gives rise to triplets (1:2:1 line intensity ratios) in the EPR spectra. ENDOR has provided information about the lattice distortion surrounding the vacancy.[27] This defect is present with slightly varying concentrations (on the order of 10^{19}-10^{20} cm^{-3}) in all samples studied.

Several additional intrinsic defects in $ZnGeP_2$ can be observed during photoexcitation. Laser excitation changes the valence of donors and acceptors, thus converting non-paramagnetic defects into paramagnetic forms. For example, phosphorus vacancies in $ZnGeP_2$ are present as singly ionized donors, but it is their neutral state which is paramagnetic.[25] These latter centers are observed by illuminating the samples with above-band-gap (514.5 nm) or below-band-gap (632.8 nm) light at temperatures below 10 K. Even at these low temperatures, the neutral state is not stable and decays back to the singly ionized form in a matter of seconds or less. The EPR spectrum from the neutral phosphorus vacancy shows no hyperfine structure, indicating the unpaired spin does not strongly interact with phosphorus neighbors. This defect is usually observed at concentrations comparable to that of the zinc vacancies.

Another native paramagnetic defect, the phosphorus antisite, is not usually seen in $ZnGeP_2$ samples grown by the horizontal gradient freeze technique. However a recently grown sample did reveal a significant concentration of this donor. Kaufmann et al.[26] initially reported the presence of phosphorus antisite centers during photoexcitation at low temperatures. This spectrum exhibits a large hyperfine splitting (about 750 G) with the central phosphorus nucleus and smaller ligand hyperfine interactions with the four nearest phosphorus neighbors. We can observe this spectrum at temperatures as high as 40 K, at which point the neutral charge state of the donor becomes unstable and converts back to its singly ionized form. This phosphorus antisite spectrum has only been present in one of the samples grown at Sanders, and for this reason it is not expected to play a major role in explaining the origin of the near-edge absorption in $ZnGeP_2$.

The optical absorption extending from 0.7 to 2.5 μm in $ZnGeP_2$ is commonly assumed to be due to point defects. We have shown that this near-edge optical absorption correlates with the intensity of the EPR spectra from singly ionized zinc vacancies. These results strongly suggest that the zinc vacancy acceptors play a direct role in the optical absorption phenomenon. Also, large concentrations of phosphorus vacancy donors were present in these samples. We conclude that the optical absorption is most likely due to several overlapping bands arising from an acceptor-to-donor transition and band-to-defect transitions. Support for this view comes from PL studies.

Results of photoluminescence experiments help to further connect these defects seen by EPR to the near infrared absorption. While PL spectra in $ZnGeP_2$ are often complex,[28] measurements taken on our samples indicate only two dominant emission bands at low temperature. One band is partially polarized along the c axis of the crystal (the 1.42 eV band) and the other band is unpolarized (the 1.62 eV band). A possible explanation for the two bands is two distinct donor-acceptor-pair (DAP) recombinations. Such a model is not considered likely since EPR data, thus far, have revealed the existence of only one dominant donor (the phosphorus vacancy) and one dominant acceptor (the zinc vacancy) in our samples. It is more likely that one of the observed bands is DAP (i.e., the 1.42-eV band) and the other is a band-to-impurity transition, i.e., an (e,A) or (D,h) transition. Since the PL spectra shown are also observed with below-band-gap light (632.8 nm), we suggest that the 1.62-eV emission is donor-hole (D,h) recombination. We find that the emission and optical absorption exhibit the same polarization behavior and, furthermore, our PL polarization study is at variance with the report of McCrae et al.[29]

A preliminary investigtion of the time-decay behavior of the PL bands has been completed. Data were obtained by monitoring the DAP emission at 1.42 eV after an 8-ns, 532-nm excitation pulse. Because of the low intensity of the emitted light, 1000 decays were accumulated. The decay occurs over a time window extending out to approximately 20 ms and can not be fit by a single exponential. These results support our previous assignment of this emission of DAP recombination in an indirect-gap semiconductor. We also measured the decay of the PL occurring at 1.62 eV and found a similar dependence on time.

EPR, ENDOR, PL, and time-resolved PL are well suited to study defects in $ZnGeP_2$. Their usefulness, however, is not restricted to studying native defects. Substitutional manganese was reported by Baran et al.,[30] and we have recently "rediscovered" this defect in material grown by the horizontal gradient freeze technique. A careful analysis of the Mn^{2+} EPR spectrum yields spin-Hamiltonian parameters similar to those reported by Baran et al. The defect is an S = 5/2 system interacting with an I = 5/2 nucleus (100% abundant). A small crystal field, due to the crystal's tetragonal symmetry, splits the spectrum into five sets of six lines. The only sample this manganese spectrum has been seen in was the one in which the phosphorus antisite was also observed. This piece was cut from the end of a boule, indicating a possible variation in stoichiometry, and photoluminescence studies have not yet been performed on this sample.

REFERENCES

1. P. F. Bordui and M. M. Fejer, Annu. Rev. Mater. Sci. 23, 321 (1993).
2. G. M. Loiacono, D. N. Loiacono, T. McGee, and M. Babb, J. Appl. Phys. 72, 2705 (1992).
3. R. Blachman, P. F. Bordui, and M. M. Fejer, Appl. Phys. Lett. 64, 1318 (1993).
4. B. Boulanger, M. M. Fejer, R. Blachman, and P. F. Bordui, Appl. Phys. Lett. 65, 2401 (1994).
5. M. P. Scripsick, D. N. Lolacono, J. Rottenberg, S. H. Goellner, L. E. Halliburton, and F. K. Hopkins, Appl. Phys. Lett. 66, 3428 (1995).
6. M. E. Hagerman and K. R. Poeppelmeier, Chem. Mater. 7, 602 (1995).

7. J. R. Quagliano, R. R. Petrin, T. C. Trujillo, R. Wenzel, L. J. Jolin, M. T. Paffett, C. J. Maggiore, N. J. Cockroft, and J. C. Jacco, in Laser-Induced Damage in Optical Materials: 1994, Proc. SPIE Vol. 2428, pp. 4-11 (1995).

8. F. Bantien, P. Albers, and G. Huber, J. Luminescence 36, 363 (1987).

9. D. Gourier, L. Colle, A. M. Lejus, D. Vivien, and R. Moncorge, J. Appl. Phys. 63, 1144 (1988).

10. W. Koechner, Solid-State Laser Engineering, 3rd edition, (Springer-Verlag, Berlin, 1992), pp. 76-77.

11. B. Henderson and G. F. Imbusch, Optical Spectroscopy of Inorganic Solids, (Clarendon Press, Oxford, 1989).

12. M. G. Roelofs, J. Appl. Phys. 65, 4976 (1989).

13. M. P. Scripsick, G. J. Edwards, L. E. Halliburton, R. F. Belt, and G. M. Loiacono, J. Appl. Phys. 76, 773 (1994).

14. I. R. Beattie and T. R. Gilson, Proc. Roy. Soc. A307, 407 (1968).

15. T. Ohsaka, F. Izumi, and Y. Pujiki, J. Raman Spectrosc. 7, 321 (1978).

16. L. S. Hsu, R. Solanki, G. J. Collins, and C. Y. She, Appl. Phys. Lett. 45, 1065 (1984).

17. M. E. Hagerman, V. L. Kozhevnikov, and K. R. Poeppelmeier, Chem. Mater. 5, 1211 (1993).

18. A. K. Ghosh, F. G. Wakim, and R. R. Addiss, Jr., Phys. Rev. 184, 979 (1969).

19. L. Grabner, S. E. Stokowski, and W. S. Brower, Jr., Phys. Rev. B 2, 590 (1970).

20. A. K. Ghosh, R. B. Lauer, and R. R. Addiss, Jr., Phys. Rev. B 8, 4842 (1973).

21. Y. Nakato, A. Tsumura, and H. Tsubomura, J. Phys. Chem. 87, 2402 (1983).

22. P. G. Schunemann, P. J. Drevinsky, M. C. Ohmer, W. C. Mitchel, and N. C. Fernelius, in Beam-Solid Interactions for Materials Synthesis and Characterization, edited by D. C. Jacobson, D. E. Luzzi, T. F. Heinz, and M. Iwaki (Mater. Res. Soc. Proc. 354, Pittsburgh, PA, 1994) pp. 729-734.

23. P. G. Schunemann, P. J. Drevinsky, and M. C. Ohmer, in Beam-Solid Interactions for Materials Synthesis and Characterization, edited by D. C. Jacobson, D. E. Luzzi, T. F. Heinz, and M. Iwaki (Mater. Res. Soc. Proc. 354, Pittsburgh, PA, 1994) pp. 579-583.

24. M. H. Rakowsky, W. K Kuhn, W. J. Lauderdale, L. E. Halliburton, G. J. Edwards, M. P. Scripsick, P. G. Schunemann, T. M. Pollak, M. C. Ohmer, and F. K. Hopkins, Appl. Phys. Lett. 64 (13), 1615 (1994).

25. N. C. Giles, L. E. Halliburton, P. G. Schunemann, and T. M. Pollak, Appl. Phys. Lett. 66, 1758 (1995).

26. U. Kaufmann, J. Schneider, and A. Räuber, Appl. Phys. Lett. 29, 312 (1976).

27. L. E. Halliburton, G. J. Edwards, M. P. Scripsick, M. P. Rakowsky, P. G. Schunemann, and T. M. Pollak, Appl. Phys. Lett. 66, 2670 (1995).

28. N. Dietz, I. Tsveybak, W. Ruderman, G. Wood, and K. J. Bachmann, Appl. Phys. Lett. 65, 2759 (1994).

29. J. E. McCrae, Jr., M. R. Gregg, R. L. Hengehold, Y. K. Yeo, P. H. Ostdiek, M. C. Ohmer, P. G. Schunemann, and T. M. Pollak, Appl. Phys. Lett. 64, 3142 (1994).

30. N. P. Baran, I. I. Tychina, I. G. Tregub, I. Yu. Tkachuk, L. I. Chernenko, and I. P. Shcherbyna, Sov. Phys. Semicond. 9, 1527 (1976).

FIGURE CAPTIONS

Figure 1. Photoluminescence from three as-grown KTP crystals. The data were taken at room temperature with cw 457-nm excitation.

Figure 2. Photoluminescence from a KTP crystal (a) in its as-grown condition, (b) at one location on the surface after a one-hour anneal at 1000°C in air, and (c) at a different location on the surface after the anneal. The original data has been multiplied by a factor of twenty in trace (a).

Figure 3. Micro-Raman from a KTP crystal (a) in its as-grown condition, (b) at one location on the surface after a one-hour anneal at 1000°C in air, and (c) at a different location on the surface after the anneal. The original data has been multiplied by a factor of two in trace (a). A single sample, annealed only once at high temperature, has been used in Figs. 2 and 3, thus allowing a direct correlation of the traces.

Figure 1

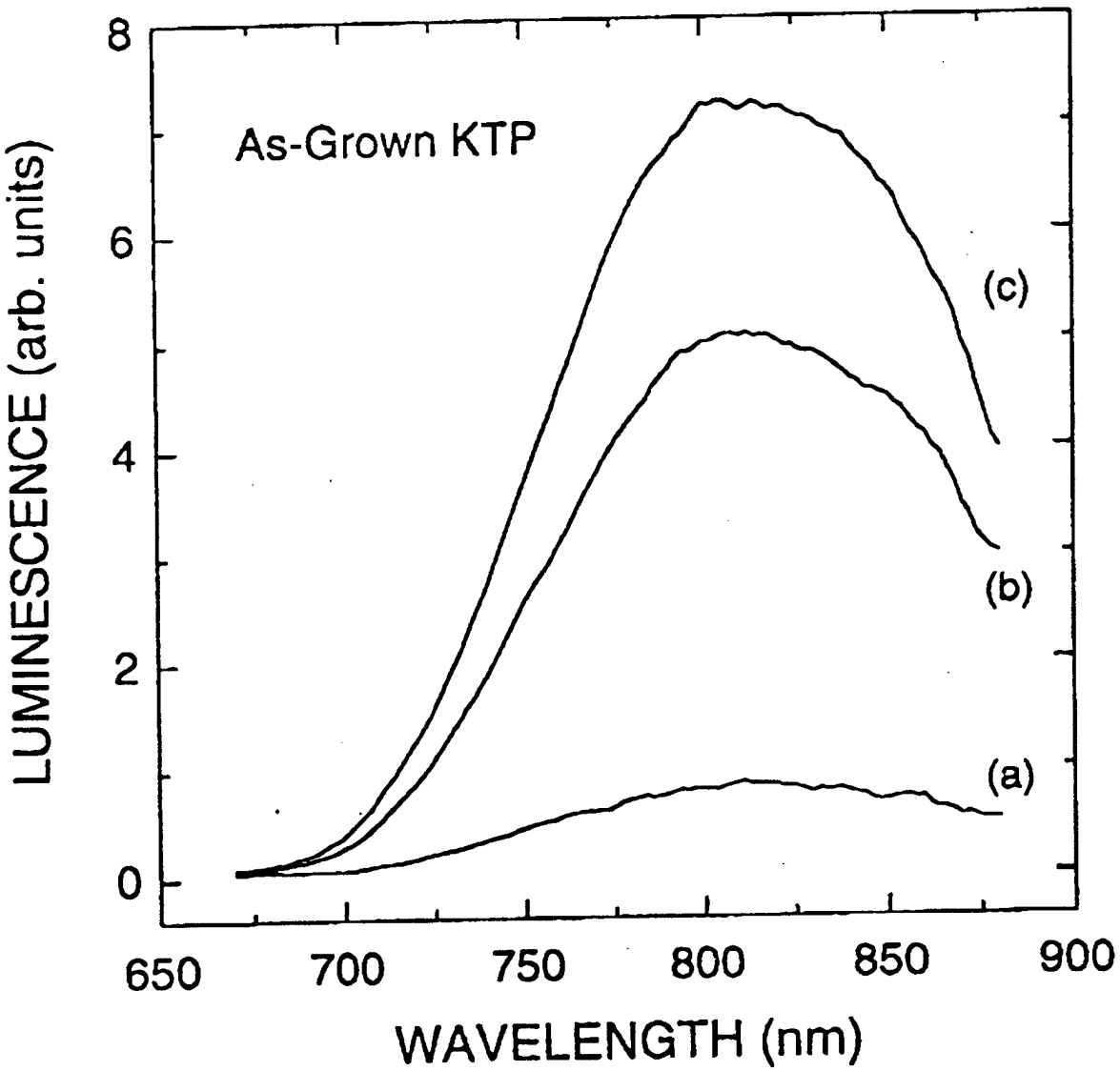
As-Grown KTP
LUMINESCENCE (arb. units)
WAVELENGTH (nm)
(a)
(b)
(c)
0
2
4
6
8
650
700
750
800
850
900

Figure 2

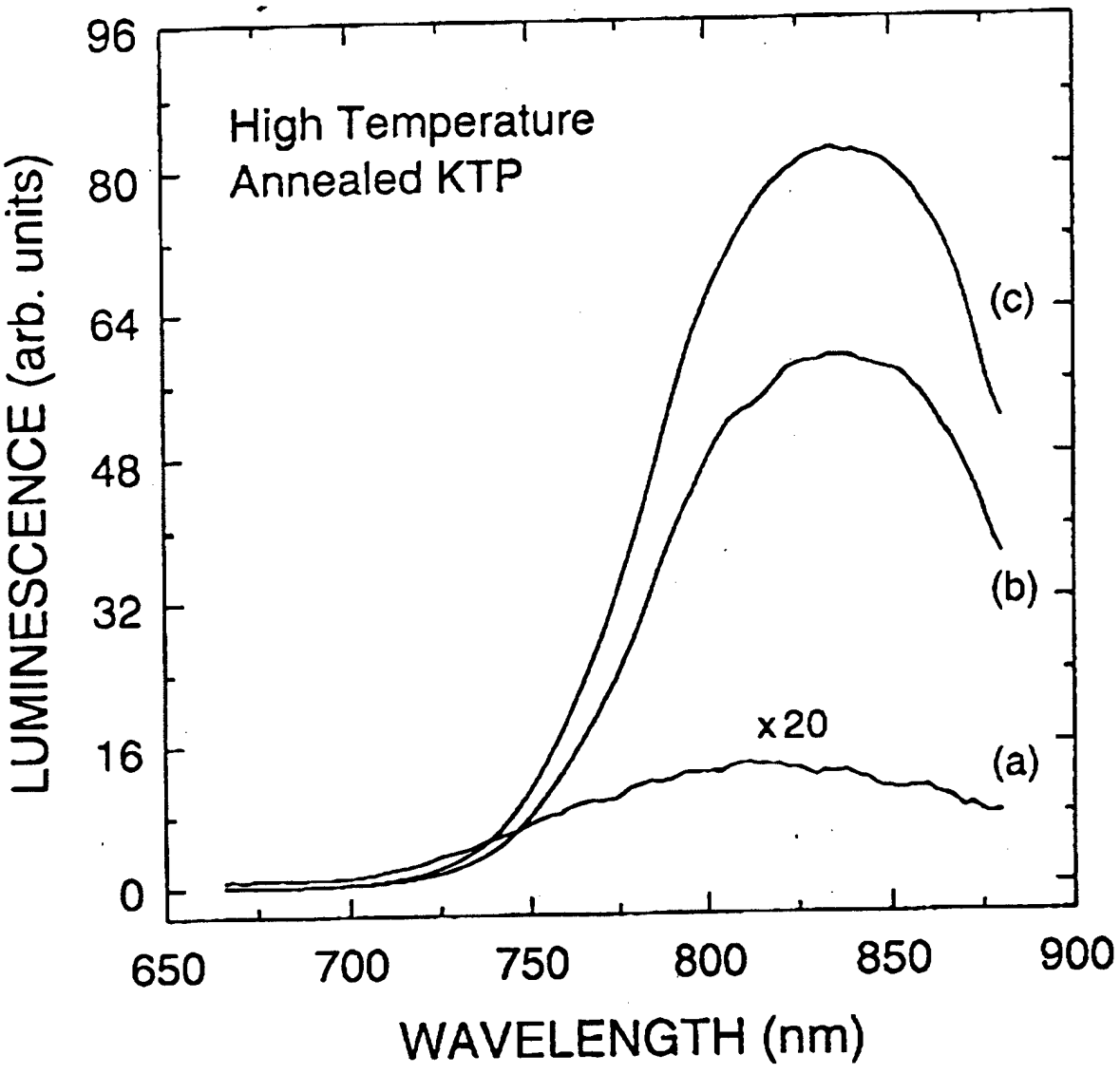
High Temperature
Annealed KTP
LUMINESCENCE (arb. units)
96
80
64
48
32
16
0
650
700
750
800
850
900
WAVELENGTH (nm)
(c)
(b)
x20
(a)

Figure 3